OSCILLATING BUBBLES RISING IN A DOUBLY CONFINED CELL

L. Pavlov*[1], M. V. D'Angelo[1], M. Cachile[1], V. Roig[2] y P. Ern[2]

[1] *Universidad de Buenos Aires, Facultad de Ingeniería, Grupo de Medios Porosos, Buenos Aires, Argentina, CONICET, Buenos Aires, Argentina.*

[2] *Institut de Mécanique des Fluides de Toulouse, Université de Toulouse and CNRS, Toulouse, France.*

Recibido: 30/10/21; Aceptado: 14/12/21

The motion of bubbles rising in confined geometries has gained interest due to its applications in mixing and mass transfer processes, ranging from bubble column reactors in the chemical industry to solar photobioreactors for algae cultivation. In this work we performed an experimental investigation of the behavior of air bubbles freely rising at high Reynolds numbers in a planar thin-gap cell of thickness $h = 2.8$ mm filled with distilled water. The in-plane width of the cell W is varied from 2.4 cm to 21 cm. We focus on the influence of lateral confinement on the motion of bubbles in the regimes with regular path and shape oscillations of large amplitude, that occur for the size range 0.6 cm $< d <$ 1.2 cm. In addition, a rise regime that consists of a vertical rise path with regular shape oscillations, that does not appear in the laterally unconfined case, is uncovered.

In the presence of lateral walls, the mean rise velocity of the bubble V_b becomes lower than the velocity of a laterally unconfined bubble of the same size beyond a critical bubble diameter d_{cV} that decreases as the confinement increases (i.e. as W decreases). The influence of the lateral confinement on the bubble mean shape can be determined from the change in the mean aspect ratio χ of the ellipse that best fits the bubble contour at each instant. It is observed that bubbles become closer to circular (χ closer to 1) as the confinement increases. The departure from the values of χ of the laterally unconfined case occur at a critical diameter $d_{c\chi}$ that is lower for greater confinement and also greater than d_{cV} for each confinement, thus indicating that the effect of the lateral confinement is seen earlier (i.e. on smaller bubbles) on the velocity than on the aspect ratio.

Assuming that the wall effect is related to the strength of the downward flow generated by the bubble, we introduce the mean flow velocity in the space let free for the liquid between the walls and the bubble, U_f, that can be estimated by mass conservation as $U_f = dV_b/(W-d)$. We further introduce the relative velocity between the bubble and the downward fluid in its vicinity $U_{rel} = V_b + U_f = V_b/\xi$, where $\xi = 1 - d/W$ is the confinement ratio of the bubble. We found that, for a given bubble size in the oscillatory regime, U_{rel} is approximately constant for all the studied values of W, and matches closely the value in the absence of lateral confinement. This provides an estimation, at leading order, of the bubble velocity that generalizes the expression proposed by Filella et al. (JFM, 2015) and accounts for the additional drag experienced by the bubble due to the lateral walls. We then show that, for given d and ξ, the frequency and amplitudes of the oscillatory motion can be predicted using the characteristic length and velocity scales d and U_{rel}.

Keywords: Bubbles, bubble kinematics, bubble shape, confined bubbles.

https://doi.org/10.31527/analesafa.2022.fluidos.66 ISSN 1850-1168 (online)

I. INTRODUCTION

The motion of bubbles freely rising in a thin-gap cell at high Reynolds numbers has interest in several fundamental and practical problems, for example in applications involving confined bubble reactors. This thin-space configuration retains the specific properties associated with inertial flows, while operating limited volumes of liquid [1-5]. In specific applications, bubbles rising in plane geometries are also limited by side walls. This work then focuses on investigating the influence of an additional transverse confinement on the bubble behavior.

The problem of a 3D bubble rising in a viscous liquid has been widely studied since the last century. The presence of walls, as in the case of a Hele-Shaw geometry, will modify the flow field around the bubble, and therefore the shape and motion of the bubble during its rise [6-8]. Introducing additional lateral walls in the cell will modify the flow around the bubble more drastically.

The inertial regime of bubbles freely rising in a thin-gap cell was investigated in detail by Roig *et al.* [9] and Filella *et al.* [10]. They highlighted the existence of different types of bubble motion and provided a characterization of the different paths observed for increasing bubble sizes. Filella *et al.* [10] proposed a simple generic estimation for the mean rise velocity of the bubble V_b valid for a large range of bubbles' sizes, $V_{b,\infty} \simeq 0.7\sqrt{gd_{eq}}$, which can also be expressed as

$$V_{b,\infty} \simeq k\ (h/d)^{1/6}\ \sqrt{gd}, \qquad (1)$$

where $k = 0.75$ and V_b is denoted $V_{b,\infty}$ for consistency with the remainder of the paper. In this expression, g is the gravitational acceleration, and the diameters

$$d_{eq} = \left(3d^2h/2\right)^{1/3} \quad \text{and} \quad d = \sqrt{4\mathscr{A}/\pi} \qquad (2)$$

are, respectively, the three-dimensional equivalent diameter of the bubble calculated with its volume (d_{eq}), and the pla-

* lpavlov@fi.uba.ar

nar equivalent diameter of the bubble determined from the area $\mathscr{A}$ covered by the bubble in the plane of the cell (d). Equation (1) indicates that the mean vertical velocity of the bubble V_b is not only proportional to the gravitational velocity $\sqrt{gd}$ but also depends on the parameter h/d imposed on the bubble by the small gap. This expression correctly describes the rise velocity of bubbles in the regimes with path and shape oscillations in cells with gap thicknesses of 1 mm [9] and 3 mm [10]. Nevertheless, it does not account for the effect of the lateral confinement on the rise velocity, which is within the scope of the present investigation.

II. EXPERIMENTAL TOOLS

The experimental apparatus consisted of a thin-gap cell of thickness $h \simeq 2.8$ mm, height H and width W_c oriented vertically and filled with distilled water. The air bubbles were released individually from a syringe connected to a nozzle located in the centre at the bottom of the cell. The experiments were performed at ambient temperature of (19 ± 1)°C, as described in Pavlov *et al.* [11]. PMMA plates were included inside the cell as internal lateral walls to reduce the effective width from W_c to W. The experiments were performed in three different cells, one made in PMMA and two made of glass plates with heights H between 30 and 50 cm and widths W_c between 9 and 21 cm. Internal walls were included, when needed, in order to reduce the effective width from W_c to $W = 9, 7, 4$ and 2.4 cm. The motion of the bubble was recorded using a high-speed camera with frame rates ranging from 150 to 1000 frames per second, and a spatial resolution between 100 and 200 μm/px, depending on the experiments. A LED backlight illumination was used to generate uniform lighting. The area, contour and centroid of the bubble were obtained using typical image processing techniques.

The behavior of the bubble can be further characterized by two Reynolds numbers [12],

$$Re = \frac{V_b d}{\nu} \quad \text{and} \quad Re_h = Re\left(\frac{h}{d}\right)^2. \tag{3}$$

The first, Re, characterizes the in-plane motion of the bubble, and the second is associated with viscous diffusion in the gap. The inertial regime, which is the focus of the present work, corresponds to both $Re \gg 1$ and $Re_h \gg 1$.

III. RESULTS AND DISCUSSION

In a previous study [11], a description of the different rise regimes is made for the case of laterally confined bubbles rising in a thin-gap cell. In this paper we will focus on the regimes with path and shape oscillations about a vertical path and also in the regime that consists of a rectilinear path with periodic shape oscillations. These regimes are presented in Fig. 1. In these regimes, an influence of lateral confinement on the average rise velocity and on the shape of the bubble is observed. The influence of the cell width W on the bubble shape can be characterized by the aspect ratio $\chi = a/b$, defined as the average over the stationary regime of the ratio between the lengths of the major and minor axes (a and b, respectively) of the ellipse that best fits the bubble contour at each time step (Fig. 2).

We are interested, in particular, in the influence of the lateral confinement on the different magnitudes that characterize the movement of the bubble, whether they are magnitudes averaged over time (such as mean velocity or aspect ratio) or magnitudes obtained from the analysis of periodic signals (such as the frequency of oscillation).

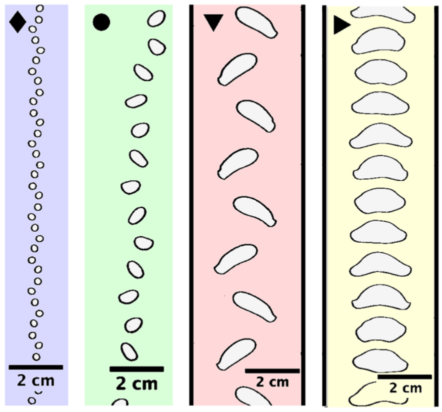

FIG. 1: Different regimes observed in the experiments (from left to right): ♢: path oscillations and moderate shape oscillations around a vertical path, ◯: path oscillations and large shape oscillations (usually with a horizontal drift in the path), ▽: path and large shape oscillations around a vertical path, ▷: rectilinear path with periodic shape oscillations.

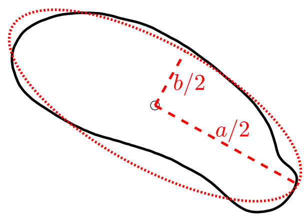

FIG. 2: Comparison of the bubble contour with the ellipse used to characterize its shape and the aspect ratio $\chi = a/b$.

An example of the studied magnitudes (instantaneous velocity and deformation) is shown in Fig. 3 for a bubble with path and shape oscillations and in Fig. 4 for the case with only shape oscillations.

The presence of the walls modifies the flow around the bubble. For sufficiently strong lateral confinement, the space available for the descent of the liquid around a rising bubble is reduced. We can define the parameter $\xi = 1 - d/W$, that compares the space let free for the downward motion of the liquid with the total width of the cell. To satisfy mass conservation, the mean downward velocity of the fluid surrounding the bubble U_f can be estimated in a first approximation from the mean bubble rise velocity V_b and the mean bubble width $\langle W_b \rangle$ as:

$$U_f = V_b \frac{\langle W_b \rangle}{W - \langle W_b \rangle}. \tag{4}$$

If we further approximate $\langle W_b \rangle$ by d (in practice, the ratio $\langle W_b \rangle / d$ takes values between 0.9 and 1.1), Eq. (4) can be

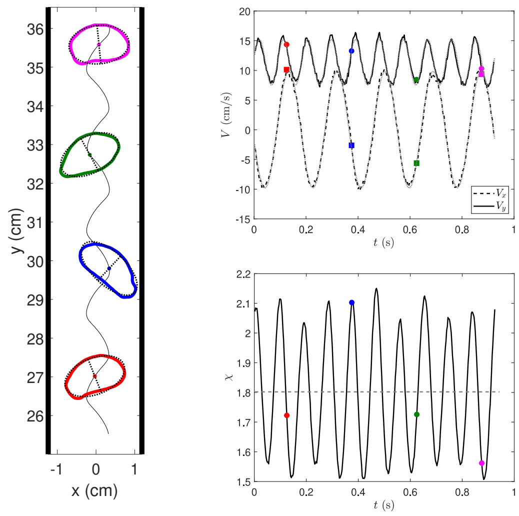

FIG. 3: Example of a bubble rising in a cell with $W = 2.4$ cm. Left: path of the center of mass of the bubble with $d = 1.09$ cm and its contours at different times. The contours are shown in colors, which serve to identify the values of the different signals at those particular instants in time. In addition, the characteristic ellipse in each case and its minor axis are shown as a gray dotted line. Top right: instantaneous velocity of the center of mass in the vertical (V_y, black solid line) or horizontal (V_x, black dashed line) direction as a function of time. The gray dotted lines correspond to fits by a sine function. Bottom right: aspect ratio χ as a function of time. The mean value of the signal is shown as a horizontal line.

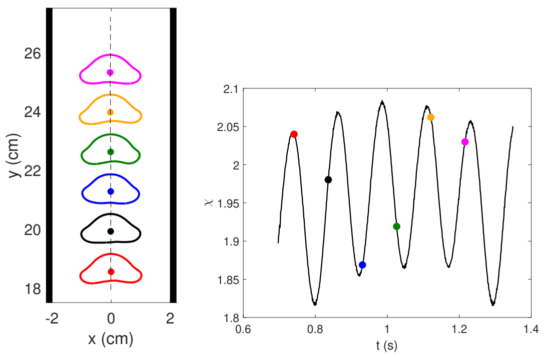

FIG. 4: Left: contours of a bubble with $d = 1.20$ cm which shows only shape oscillations, at different times. Right: aspect ratio χ as a function of time for this bubble.

written as:

$$U_f = V_b \frac{d}{W - d}. \tag{5}$$

A mean relative velocity between the bubble and the liquid can then be introduced as

$$U_{rel} = V_b + U_f = V_b \frac{W}{W - d} = \frac{V_b}{\xi}. \tag{6}$$

Fig. 5 shows both V_b and U_{rel} as a function of d for the different lateral confinements. As can be seen, while the mean rise velocity V_b is lower for stronger lateral confinements, the values of U_{rel} are located in a single curve for all the studied values of W. This indicates that a bubble of a given size in these regimes always rises with the same value of U_{rel}, regardless of the lateral confinement. Therefore, ξ

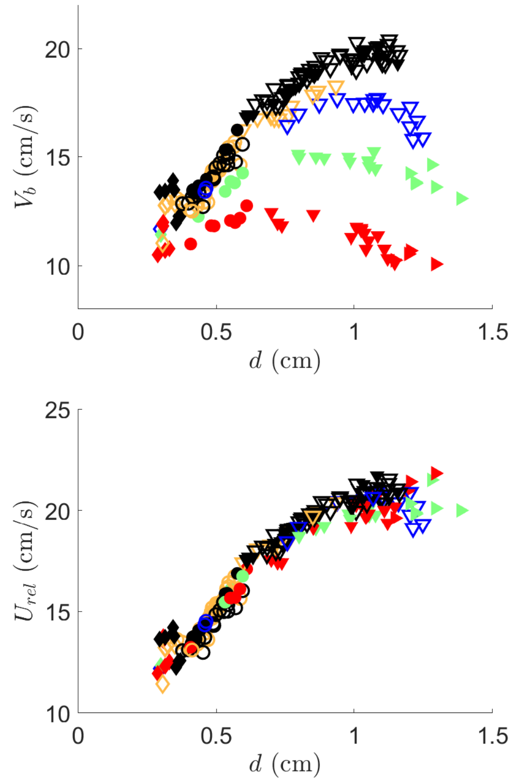

FIG. 5: Bubble mean rise velocity (top) and mean relative velocity between the bubble and the surrounding fluid (bottom), as a function of d. The color of the data points is associated with the value of the cell width W (empty black: $W = 21$ cm, filled black: $W = 15$ cm, orange: $W = 9$ cm, blue: $W = 7$ cm, green: $W = 4$ cm, red: $W = 2.4$ cm), and each symbol (being it empty or filled) represents a rise regime (see Fig. 1).

is a parameter that quantifies, in the studied regimes, how much slower a bubble of diameter d rises in a cell of width W with respect to the velocity that the same bubble would have in the absence of lateral confinement. In the limit of no lateral confinement, $\xi \Longrightarrow 1$, and thus $U_{rel} \simeq V_{b,\infty}$, which can be used to generalize equation (1) in order to account for the lateral confinement [13].

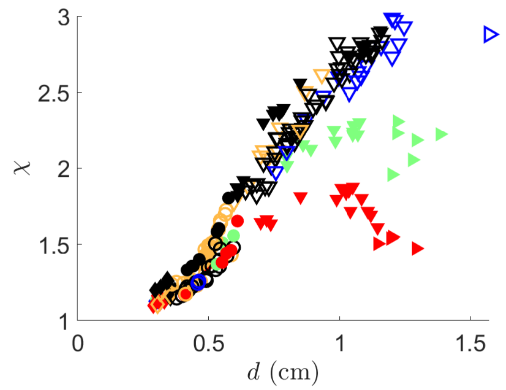

FIG. 6: χ as a function of d. The symbol convention is the same as in Fig. 5.

For a given bubble size, a stronger confinement also produces less elongated shapes, *i.e.*, χ closer to unity (Fig. 6). The effect of confinement, that is, the departure from the unconfined case (which can be taken as the $W = 21$ cm case [11]) occurs for smaller bubble sizes in the case of the mean rise velocity as compared with the mean aspect ratio of the bubble. This can be particularly noticed in the $W = 7$ cm case, for which the departure from the mean rise velocity of unconfined occurs already at $d \approx 0.7$ cm, while for bubbles of that size the value of χ is the same in that confinement as compared with the unconfined case. More generally, if one defines $d_{cV}(W)$ (resp. $d_{c\chi}(W)$) as the diameter for which the effect of the confinement begins to be noticed in V_b (resp. χ) for a given W, then $d_{cV}(W) < d_{c\chi}(W)$.

For sufficiently confined bubbles, there is a small size range for which the bubble rises with shape oscillations but with a vertical center of mass trajectory. This regime is not observed in the unconfined case because the trajectory of the bubble eventually becomes unstable and begins to show oscillations, which may or may not be regular. The lateral confinement thus provides a stabilizing effect to the movement of the bubble in this scenario.

For bubbles with both path and shape oscillations the fundamental frequency f is that corresponding to the path oscillations. This frequency, f is related with the frequency f_χ, corresponding to shape oscillations, being $f = f_\chi/2$ (Fig. 3). This indicates that the bubble aspect ratio has two oscillations at every period of path oscillation, which in turn reflects the symmetry of the path. In contrast, in the case of bubbles that only have shape oscillations the only frequency will be f_χ. We present, then, in Fig. 7 the frequency values corresponding to the shape oscillations, for all the bubbles studied in this work.

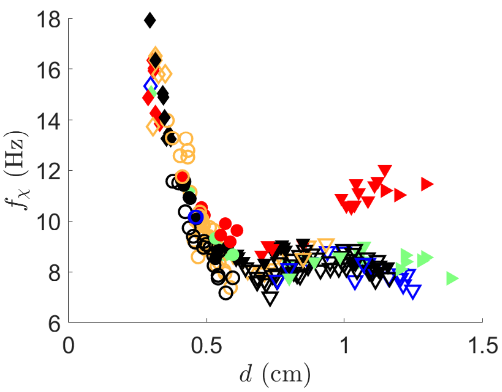

FIG. 7: Frequency f_χ as a function of d. The symbol convention is the same as in Fig. 5.

For each W, the values of f_χ for bubbles in the regime of only shape oscillations are close to those of the biggest bubbles showing path oscillations. This means that, even if the characteristics of the rise regime are completely different, the frequency of the shape oscillations does not change between the two regimes.

Moreover, the frequency of oscillation does not depend on the cell width (except for the most confined cases, $\xi < 0.6$, for which a "bouncing" effect appears [11]). The same can be said for the amplitude of oscillation of the vertical component of the velocity (Fig. 8). This means that the characteristic velocity scale that controls those parameters is the relative velocity between the bubble and the fluid and not the bubble mean rise velocity [11].

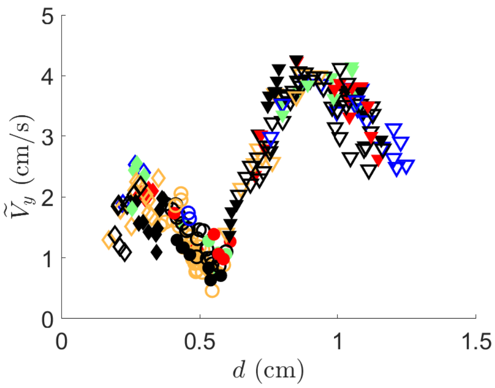

FIG. 8: Amplitude of oscillation of the vertical component of the velocity, V_y, as a function of d. The symbol convention is the same as in Fig. 5.

It is interesting to point out some similarities between the laterally confined cases and the problem of a bubble rising in a thin-gap cell that is laterally unbounded, in the presence of a moderate counterflow. In that problem, it was found [14] that the bubble velocity slows down in the presence of a counterflow of mean velocity U_{cf}, its final rise velocity being $V_b - U_{cf}$ (where U_{cf} was always smaller than V_b). This means that the mean relative velocity between the bubble and the fluid remains unchanged with respect to the case of the bubble rising freely (in the absence of counterflow), as it is the case in the laterally confined cases. Moreover, the velocity amplitudes and frequency of oscillation also remain the same regardless of the counterflow, as it is the case with the lateral confinement. However, some differences arise, particularly with respect to the bubble shape. The presence of a counterflow barely modifies the mean aspect ratio χ of the bubble, while it was seen (Fig. 6) that the lateral confinement produces a decrease in the value of χ for a bubble of a given size. A similar behavior can be seen in the amplitude of the orientation of the bubble (not shown in this work), which is in fact a magnitude that is strongly related to χ [11].

IV. CONCLUSIONS

We investigated the oscillatory motion of inertial bubbles rising in a thin-gap cell with an additional lateral confinement. The influence of the cell width W on the bubble rise velocity, shape and oscillations was characterized. A mean relative velocity between the bubble and the fluid was introduced and shown to be independent of W. The analogy with the results for a counterflow experiment without lateral confinement was discussed. Finally, for strong enough lateral confinements we also showed the existence of a regime for which the bubble exhibits only shape oscillations.

ACKNOWLEDGMENTS

The authors are grateful to G. Ehses, G. Albert and L. Mouneix for building the IMFT experimental set-up and to S. Cazin for his help with the optical technique. This collaboration was possible thanks to the financial support from CONICET and Universidad de Buenos Aires, Argentina and from INPT, Toulouse (SMI fundings 2016 and 2018) and became part of the IRP CNRS-CONICET IVMF in

2019.

REFERENCES

[1] E. Alméras, F. Risso, V. Roig, P. C. y F. Augier. Mixing mechanism in a two-dimensional bubble column. Phys. Rev. Fluids **3,** 074307 (2018).

[2] M. Roudet, A.-M. Billet, S. Cazin, F. Risso y V. Roig. Experimental investigation of interfacial mass transfer mechanisms for a confined high Reynolds-number bubble rising in a thin gap. AIChE Journal **63,** 2394-2408 (2017).

[3] C. Thobie, E. Gadoin, W. Blel, J. Pruvost y C. Gentric. Global characterization of hydrodynamics and gas-liquid mass transfer in a thin-gap bubble column intended for microalgae cultivation. Chemical Engineering & Processing: Process Intensification **122,** 76-89 (2017).

[4] F. Felis, F. Strassl, L. Laurini, N. Dietrich, A.-M. Billet, V. Roig, S. Herres-Pawlis y L. K. Using a bio-inspired copper complex to investigate reactive mass transfer around an oxygen bubble rising freely in a thin-gap cell. Chem. Eng. Sci. **207,** 1256-1269 (2019).

[5] Z. Zhang, H. Zhang, X. Yuan y K.-T. Yu. Effective uv-induced fluorescence method for investigating interphase mass transfer of single bubble rising in the Hele-Shaw cell. Industrial & Engineering Chemistry Research **59,** 6729-6740 (2020).

[6] F. Takemura, S. S. Takagi, J. Magnaudet e Y. Matsumoto. Drag and lift forces on a bubble rising near a vertical wall in a viscous liquid. J. Fluid Mech. **461,** 277-300 (2002).

[7] F. Takemura y J. Magnaudet. The transverse force on clean and contaminated bubbles rising near a vertical wall at moderate Reynolds number. J. Fluid Mech. **495,** 235-253 (2003).

[8] H. Jeong y H. Park. Near-wall rising behaviour of a deformable bubble at high Reynolds number. J. Fluid Mech. **771,** 564 (2015).

[9] V. Roig, M. Roudet, F. Risso y A.-M. Billet. Dynamics of a high-Reynolds-number bubble rising within a thin gap. J. Fluid Mech. **707,** 444-466 (2012).

[10] A. Filella, P. Ern y V. Roig. Oscillatory motion and wake of a bubble rising in a thin-gap cell. J. Fluid Mech. **778,** 60 (2015).

[11] L. Pavlov, M. V. D'Angelo, M. Cachile, V. Roig y P. Ern. Kinematics of a bubble freely rising in a thin-gap cell with additional in-plane confinement. Phys Rev. Fluids **6,** 093605 (2021).

[12] J. Bush e I. Eames. Fluid displacement by high Reynolds number bubble motion in a thin gap. Int. J. Multiphase Flow **24,** 411 (1998).

[13] L. Pavlov, S. Cazin, P. Ern y V. Roig. Exploration by Shake-the-Box technique of the 3D perturbation induced by a bubble rising in a thin-gap cell. Exp. Fluids **62** (ene. de 2021).

[14] A. Filella. *Mouvement et sillage de bulles isolées ou en interaction confinées entre deux plaques* Tesis doct. (Université de Toulouse, 2015).